Heliyon 8 (2022) e09470

Contents lists available at ScienceDirect

Heliyon

journal homepage: www.cell.com/heliyon

Research article

Novel ferrocene imide derivatives: synthesis, conformational analysis and X-ray structure

Mojca Čakić Semenčić [a,*], Ivan Kodrin [b,**], Krešimir Molčanov [c], Monika Kovačević [a], Vladimir Rapić [a]

[a] Department of Chemistry and Biochemistry, Faculty of Food Technology and Biotechnology, University of Zagreb, Pierottijeva 6, Zagreb, Croatia
[b] Department of Chemistry, Faculty of Science, University of Zagreb, Horvatovac 102a, 10000 Zagreb, Croatia
[c] Division of Physical Chemistry, Ruđer Bošković Institute, Bijenička cesta 54, Zagreb, Croatia

GRAPHICAL ABSTRACT

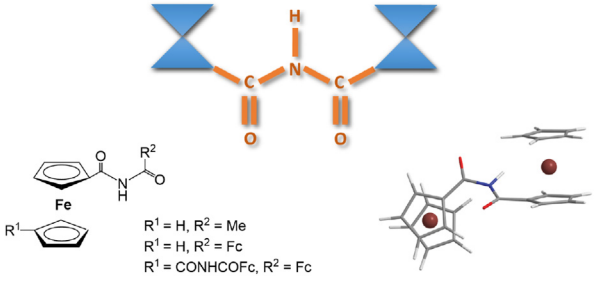

ARTICLE INFO

Keywords:
Conformational analysis
Crystal structure
DFT study
Ferrocene
Foldamers
Imide

ABSTRACT

The synthesis and structural characterization of the ferrocene imide derivatives Fc−CO−NH−CO−Me (**4**), Fc−CO−NH−CO−Fc (**7**) and Fc−CO−NH−CO−Fn−CO−NH−CO−Fc (**8**) have been reported. The mononuclear, dinuclear and trinuclear ferrocene imides were prepared by the reaction of ferrocenecarboxamide (**3**), with acetyl chloride, ferrocenecarbonyl chloride (**2**) and ferrocene-1,1'-(dicarbonyl chloride) (**6**), respectively. IR spectroscopic analysis revealed the absence of intramolecular hydrogen bonds in solutions of imides **4**, **7** and **8**. The crystal packing of *N*-acetylferrocenecarboxamide (**4**) is characterized by N−H···O hydrogen bonds forming centrosymmetric dimers, while the molecules of its homologue *N*-methylferrocenecarboxamide (**5**) are self-assembled by intermolecular N−H···O bonds into infinite chains. A detailed conformational analysis (DFT study) suggests the *cis-trans* configuration of ferrocene imide derivative **7** in solution. The effect of different substituents attached to bridged imide nitrogen on conformational properties of bis-ferrocenyl imides was further investigated and results compared to the existing experimental data.

* Corresponding author.
** Corresponding author.
E-mail addresses: mcakic@pbf.hr (M.Č. Semenčić), ikodrin@chem.pmf.hr (I. Kodrin).

https://doi.org/10.1016/j.heliyon.2022.e09470
Received 17 February 2022; Received in revised form 22 March 2022; Accepted 13 May 2022

1. Introduction

Aromatic foldamers are architectures constructed by linking aromatic monomers with various linkers such as urea [1], guanidine [2], or most commonly amide spacers [3, 4]. The folding properties of these molecules depend on noncovalent interactions and the conformational properties of the linker, which are determined by steric and electronic factors [5]. The high stability of the folded structures and the predictability of the folding patterns are remarkable properties of these "abiotic" foldamers [6]. Although several foldamers containing various aromatic subunits and spacers have been prepared, literature data dealing with those containing imide linkers are limited [7, 8, 9, 10, 11]. One of the first examples of a foldamer containing naphthalene rings linked with an imido group that forces the aromatic rings to be placed in the positions facing each other and allows π-stacking interactions was given by Kohmoto and co-workers [11]. The folding of this system into predominantly one helix was achieved by introducing a chiral centre at the nitrogen atom of the imido-carbonyl spacer and confirmed by electronic circular dichroism (ECD) spectroscopy. Our group has reported the synthesis and structural studies of bis- and tris-ferrocenyl imide foldamers Fc−CO−NMe−CO−Fc (**I**) and Fc−CO−NMe−CO−Fn−CO−NMe−CO−Fc (**II**), where the presence of a simple *N*-methyl substitution of the imido bridges efficiently induces the formation of helical conformations [12]. Due to favourable π-stacking and C−H•••π interactions between the ferrocenyl units and steric factors, *cis-cis* conformations are present both in the solid state and in solution of **I** and **II**, rather than an energetically favourable *cis-trans* conformations found in simple acyclic imides [13, 14]. A twisted imide bond (*cis-cis*) was also reported in the crystal structure of the novel noncyclic imide derived from 4-chloroaniline and 2-furoic acid [15]. The nonplanarity of the imide group was related to the steric hindrances of the 2-carbonyl furan rings. Recently, a few papers were focused on a conformational analysis of structurally very similar compounds derived from ureas. *N*-Acyl urea compounds, R–CO−NH−CO−NH−R, when compared to basic imides, R–CO−NH−CO−R, have an additional NH group [16, 17]. However, this NH group may form six-membered ring via intermolecular hydrogen bond, N−H···OC, thus initiating very similar relative orientation of the rest of the fragment as reported in *cis-trans* stereoisomers of imides.

The ferrocene-containing imide bridged systems are even rarer than similar aromatic counterparts. Among the already mentioned bis-ferrocenyl imide compound with methylated imide group [12], there are only two other similar systems. The first has phenyl group [18], and the second pyridyl group [19, 20] on the imide nitrogen atom. Continuing the study of poorly described aromatic systems with imide linkers, we have synthesized the derivatives Fc−CO−NH−CO−Me (**4**), Fc−CO−NH−CO−Fc (**7**), and Fc−CO−NH−CO−Fn−CO−NH−CO−Fc (**8**), which are the lowest homologues of ferrocene foldamer sequences. Prior to our study, we had expected that the NH hydrogen bond donor in the imide linker of the trinuclear derivative **8** might initiate hydrogen bond formation and consequently different, presumably helical, conformational outcomes compared to other reported *N*-substituted imide derivatives.

2. Experimental

The syntheses were carried out under an argon atmosphere. The toluene, dichloromethane and dioxane used for the synthesis were dried (CaH_2) and freshly distilled before use. The products were purified by preparative thin layer chromatography on silica gel (Merck, silica gel $60HF_{254}$) using EtOAc, CH_2Cl_2/EtOAc and CH_2Cl_2/EtOH as eluents. Melting points were determined using a Reichert Thermovar HT1 BT 11 melting point apparatus. IR spectra were recorded as CH_2Cl_2 solutions and KBr pellets using a Bomem MB 100 mid FTIR spectrophotometer. ^1H and ^{13}C NMR spectra were recorded using a Varian Gemini 300 spectrometer in $CDCl_3$ solution with Me_4Si as internal standard. HR-EI mass spectra (MS) were recorded on a JEOL JMS-700. Elemental analyses were performed by the analytical laboratory of the department of physical chemistry, Ruđer Bošković Institute. Starting compounds ferrocenecarboxylic acid (**1**), ferrocenecarbonyl chloride (**2**) [21], ferrocene-1, 1′-dicarbonyl chloride (**6**) [22], and *N*-methylferrocenecarboxamide (**5**) [23], were prepared according to the previously described procedures.

Table 1. Crystallographic data, collection, and structure refinement details for **4** and **5**.

Compound	4	5
Empirical formula	$C_{13}H_{13}FeNO_2$	$C_{12}H_{13}FeNO$
Formula wt./g mol^{-1}	271.09	243.08
Crystal dimensions/mm	0.22 × 0.20 × 0.18	0.25 × 0.20 × 0.20
Space group	$P\,2_1/c$	$P\,\bar{1}$
a/Å	7.37810 (10)	10.1461 (4)
b/Å	7.6572 (2)	10.1635 (5)
c/Å	20.3958 (4)	10.9934 (4)
α/°	90	103.531 (4)
β/°	91.107 (2)	105.935 (4)
γ/°	90	90.024 (4)
Z	4	4
V/Å^3	1152.06 (4)	1057.28 (8)
D_{calc}/g cm^{-3}	1.563	1.527
μ/mm^{-1}	10.402	11.185
Θ range/°	4.34–76.05	4.31–76.52
T/K	293 (2)	293 (2)
Diffractometer type	Xcalibur Nova	Xcalibur Nova
Range of h, k, l	$-9 < h < 8$	$-12 < h < 8$
	$-9 < k < 9$	$-12 < k < 12$
	$-17 < l < 25$	$-11 < l < 13$
Reflections collected	5384	9547
Independent reflections	2370	4375
Observed reflections ($I \geq 2\sigma$)	2072	3672
Absorption correction	Multi-scan	Multi-scan
R_{int}	0.0284	0.0343
R (F)	0.0339	0.0405
R_w (F^2)	0.1056	0.1225
Goodness of fit	1.026	1.069
H atom treatment	Constrained	Constrained
No. of parameters	154	271
$\Delta\rho_{max}$, $\Delta\rho_{min}$ (eÅ^{-3})	0.317; −0.299	0.526; −0.498

Ferrocenecarboxamide (3) A solution of ferrocenecarbonyl chloride (**2**) (331 mg; 1.332 mmol) in a dry toluene was cooled to 0 °C and treated with gaseous NH_3 for 2 h at room temperature. The mixture was evaporated to dryness *in vacuo*, dissolved in ethyl acetate and washed with water and brine, dried over anhydrous sodium sulphate, and evaporated to dryness *in vacuo* to give 300 mg (98%) orange crystals of **3**. m.p. = 163–165 °C. IR (CH_2Cl_2) ν_{max}/cm^{-1}: 3410 (NH), 1668 (CO), 1586 (NH).

***N*-Acetylferrocenecarboxamide (4)** A solution of **3** (37 mg; 0.161 mmol) in dry dioxane (3 ml) was dropped into a stirred suspension of hexane-washed sodium hydride (60% in mineral oil, 18 mg, 0.467 mmol) in dry dioxane (2 ml). After heating at 120 °C for 2 h, the mixture was cooled to 0 °C and a solution of acetyl chloride (0.02 ml; 0.258 mmol) in dry dioxane (4 ml) was added. The mixture was stirred overnight at room temperature. The solvent was removed, and the residue was dissolved in dichloromethane, washed with water and brine, dried over anhydrous sodium sulphate, and evaporated to dryness *in vacuo*. The crude product was purified by TLC on silica gel plates with ethyl acetate as eluent to give 34.7 mg (80%) orange crystals of **4**. m.p. = 149–152 °C. IR (CH_2Cl_2) ν_{max}/cm^{-1}: 3400 m (N−H_{free}), 1713 m, 1696 s (C=O). ^1H NMR ($CDCl_3$) δ/ppm: 2.59 (s, 3H, CH_3), 4.25 (bs, 5H, Cp−$H_{unsub.}$), 4.51 (bs, 2H H_3/H_4), 4.82 (bs, 2H, H_2/H_5), 8.56 (s, 1H, NH). ^{13}C NMR δ/ppm: 25.5 (CH_3), 69.0 (2C, C_3/C_4), 70.2 (5C, $Cp_{unsub.}$), 72.2 (2C, C_2/C_5), 73.3 (C_1), 169.9

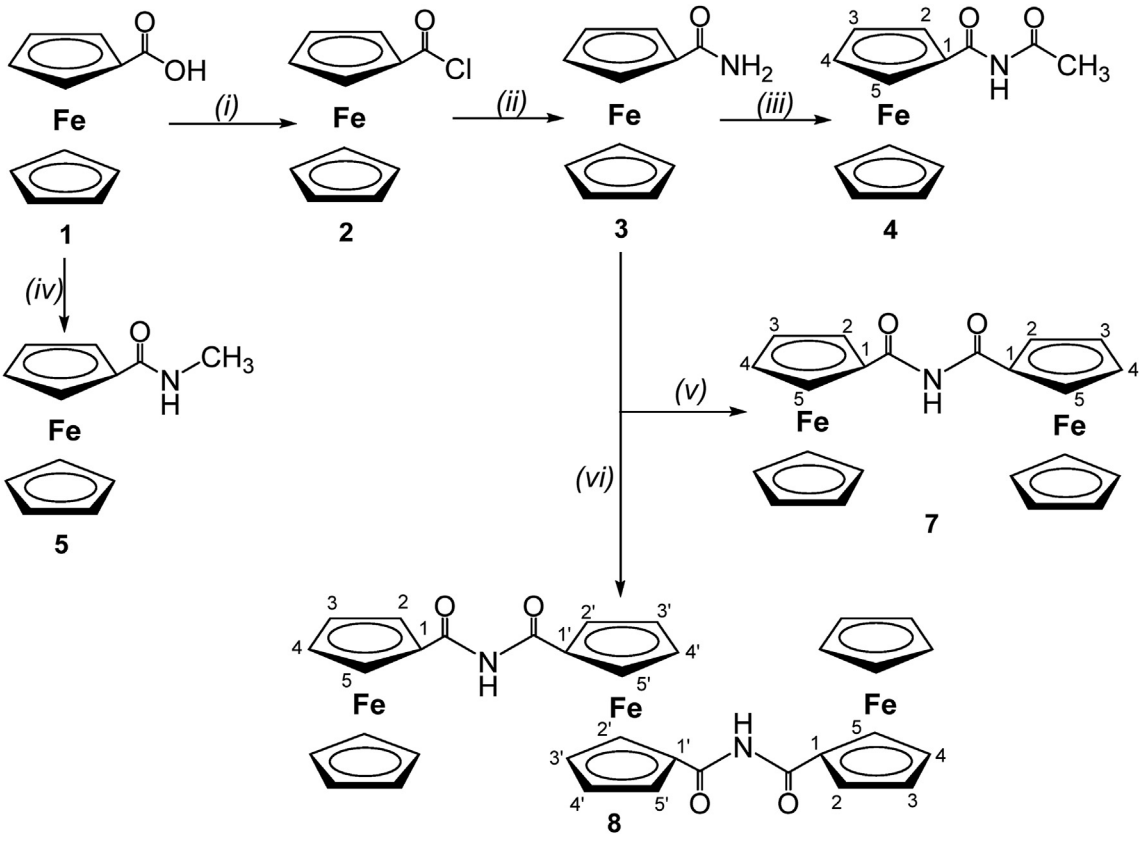

Scheme 1. Synthesis of mononuclear (**4**), dinuclear (**7**) and trinuclear (**8**) ferrocene imides. More details can be found in the Experimental section. (*i*) $(COCl)_2$, Py, dry CH_2Cl_2, reflux 2½ h, (*ii*) $NH_{3(g)}$, dry toluene, r.t. 2 h, (*iii*) CH_3COCl, NaH, dioxane, r.t. 1½ h, (*iv*) 1. HOBt/EDC, dry CH_2Cl_2, 2. $CH_3NH_2 \cdot HCl/Et_3N$, *(v)* FcCOCl (**2**), NaH, dioxane, r.t. 1½ h, *(vi)* $Fn(COCl)_2$ (**6**), NaH, dioxane, r.t. overnight.

(C=O), 173.3 (C=O). HRMS(EI): calcd. for $C_{13}H_{13}FeNO_2$, 271.0296; found 271.0288. Anal. Calcd. for $C_{13}H_{13}FeNO_2$ (271.10): C57.60, H4.83, N5.17; found C57.89, H4.87, N5.13.

***N*-Ferrocenoylferrocenecarboxamide (7)** Compound **3** (72 mg; 0.314 mmol) was activated with sodium hydride as described previously and after heating at 120 °C for 2 h, the mixture was cooled to 0 °C and a solution of ferrocenecarbonyl chloride (**2**) (78 mg; 0.314 mmol) in dry dioxane was added. The mixture was stirred for 2 h at room temperature. The solvent was removed, and the residue was dissolved in dichloromethane, washed with water and brine, dried over anhydrous sodium sulphate, and evaporated to dryness *in vacuo*. The crude product was TLC purified with dichloromethane/ethyl acetate (10:1) mixture as eluent on silica gel plates to afford 72 mg (52%) orange crystals of **7**. m.p. 216–219 °C. IR (CH_2Cl_2) ν_{max}/cm^{-1}: 3450 w (N−H_{free}), 1733 s, 1677 m (C=O). ^1H NMR ($CDCl_3$) δ/ppm: 4.33 (bs, 10H, Cp−$H_{unsub.}$), 4.53 (bs, 4H, H_3/H_4), 4.84 (bs, 4H, H_2/H_5), 8.37 (s, 1H, NH). ^{13}C NMR δ/ppm: 69.0 (4C, C_3/C_4), 70.2 (10C, $Cp_{unsub.}$), 71.9 (4C, C_2/C_5), 74.3 (2C, C_1), 168.2 (C=O). HRMS(EI): calcd. for $C_{22}H_{19}Fe_2NO_2$, 441.0114; found 441.0125. Anal. Calcd. for $C_{22}H_{19}Fe_2NO_2$ (551.09): C59.91, H4.34, N3.18; found C60.07, H4.38, N3.21.

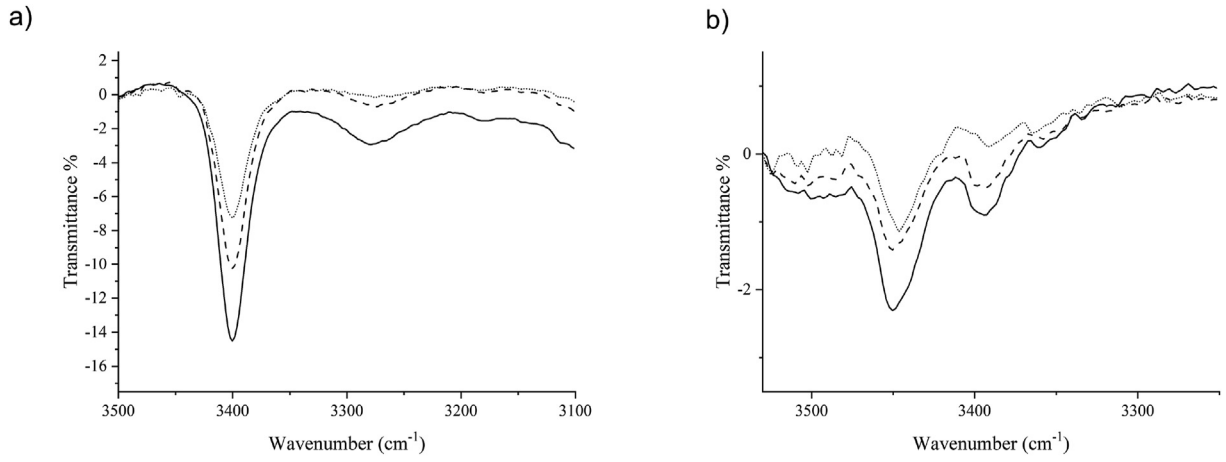

Figure 1. The NH stretching vibrations in concentration-dependent IR spectra of compounds **4** (a) and **7** (b) in the range from $c = 5 \times 10^{-2}$ mol dm^{-3} (solid line) to 1×10^{-3} mol dm^{-3} (dotted line). More details in Supporting information.

Table 2. The stretching vibrations, ^{1}H NMR signals and $\Delta\delta^a$ values of NH groups of **4**, **5**, **7** and **8**.

	ν NH_{free} (cm^{-1})		ν $NH_{assoc.}$ (cm^{-1})		δ NH	$\Delta\delta^a$
	CH_2Cl_2	KBr	CH_2Cl_2	KBr	(ppm)	(ppm)
4	3400 m	-	3276 vw	3354 w 3309 w	8.56	0.04
5	3463 w	-	-	3298 m	5.91	
7	3450 w	-	3393 vw	3349 w 3307 w	8.37	0.10
8	3412 w	-	-	3348 vw 3309 vw	8.68	0.04

[a] $\Delta\delta$ (ppm) = $\delta(CDCl_3, c = 1 \times 10^{-2}$ mol $dm^{-3}) - \delta(CDCl_3, c = 1 \times 10^{-3}$ mol $dm^{-3})$.

***N,N'*-(Ferrocene-1,1′-dicarbonyl)bisferrocenecarboxamide (8)** Compound **3** (420 mg; 1.833 mmol) was activated with sodium hydride as previously described and after heating at 120 °C for 5 h, the mixture was cooled to 0 °C and a solution of ferrocene-1,1′-dicarbonyl chloride (**6**) (268 mg; 0.863 mmol) in dry dioxane was added. The mixture was stirred overnight at 64 °C. The solvent was removed, and the residue was dissolved in dichloromethane. After aqueous workup, the organic layer was evaporated to dryness in vacuo, which gave 112.6 mg (19%) orange crystals of **8** after TLC purification with dichloromethane/ethanol (10:1) mixture as eluent. m.p. > 230 °C (decomposition). IR (CH_2Cl_2) ν_{max}/cm^{-1}: 3412 w (N−H_{free}), 1727 s, 1671 m (C=O). ^{1}H NMR ($CDCl_3$) δ/ppm: 4.37 (bs, 10H, Cp−$H_{unsub.}$), 4.57 (pt, 4H, H_3/H_4), 4.65 (pt, 4H, $H_{3'}/H_{4'}$), 4.86 (pt, 4H, H_2/H_5), 5.02 (pt, 4H, $H_{2'}/H_{5'}$), 8.68 (s, 2H, NH). ^{13}C NMR δ/ppm: 69.4 (4C, C_3/C_4), 70.2 (10C, $Cp_{unsub.}$), 70.9 (2C, C_1), 72.1 (8C, $C_{3'}/C_{4'}$, C_2/C_5), 72.9 (4C, $C_{2'}/C_{5'}$), 74.3 (2C, $C_{1'}$), 168.6 (C=O), 169.0 (C=O). HRMS(EI): calcd. for $C_{34}H_{28}Fe_3N_2O_4$, 696.0097; found 696.0089. Anal. Calcd for $C_{34}H_{28}Fe_3N_2O_4$ (696.15): C58.66, H4.05, N4.02; found C58.87, H4.13, N4.09.

2.1. X-ray diffraction

Single crystal measurements were performed on an Oxford Diffraction Xcalibur Nova R (CCD detector, microfocus Cu-tube). Program package CrysAlis PRO [24] was used for data reduction. The structures were solved using SHELXS97 [25] and refined with SHELXL97 [25]. Models were refined using the full-matrix least squares refinement; all non-hydrogen atoms were refined anisotropically. Hydrogen atoms were treated as constrained entities, using the command AFIX in SHELXL97 [25]. Molecular geometry calculations were performed by PLATON [26], and molecular graphics were prepared by CCDC-Mercury software [27]. Crystallographic and refinement data for the structures reported in this paper are shown in Table 1.

2.2. Computational details

Conformational analysis was performed in three stages for each of the five compounds (**4**, **5**, **7**, **9** and **10**). This approach was already used in many of our investigations regarding mono- and disubstituted ferrocenes [28, 29, 30, 31, 32, 33, 34, 35, 36, 37]. Low-level optimizations were performed in MacroModel [38, 39] and OPLS2005 force field was used with different search algorithms to obtain the best set of geometries at the molecular mechanics level of theory. A series of the most stable conformers were further optimized in Gaussian16 [40] on the B3LYP-D3/LanL2DZ level of theory. In the last stage, set of the most stable conformers from a previous step were submitted to full optimizations in chloroform modelled as polarizable continuum (SMD model, chloroform) at the B3LYP-D3/6-311+G (d,p) level of theory while LanL2DZ was used for Fe. Vibrational analysis was performed to verify each structure as a minimum on the potential energy surface. Reported energies refer to standard Gibbs free energies at 298 K calculated relative to the energy of the most stable conformer in chloroform for each series of the investigated compounds.

Table 3. Selected torsion angles (in deg) defining the orientation of the substituted amide group in compounds **4** and **5.**

	4	5A	5B
N (1)–C (1)–C (2)–C (3)	−164.0 (2)	17.5 (5)	162.5 (3)
C (12)–N (1)–C (1)–C (2)	−173.5 (2)	−175.6 (3)	−175.2 (3)
C (12)–N (1)–C (1)–O (1)	7.6 (4)	1.0 (5)	1.6 (5)

3. Results and discussion

3.1. Synthesis of ferrocene imides

The synthesis of the target ferrocene imides Fc−CO−NH−CO−Me (**4**), Fc−CO−NH−CO−Fc (**7**) and Fc−CO−NH−CO−Fn−CO−NH−CO−Fc (**8**) is shown in Scheme 1. Ferrocenecarbonyl chloride (**2**), obtained from ferrocenecarboxylic acid (**1**) by a standard procedure described in the literature, was treated with gaseous ammonia to give ferrocenecarboxamide (**3**) [41]. Addition of 1.5 mol of acetyl chloride or 1 mol of ferrocenecarbonyl chloride (**2**) or 0.5 mol of ferrocene-1, 1′-dicarbonyl chloride (**6**) to the cooled suspension of ferrocenecarboxamide sodium salt (obtained by heating with a large molar excess of NaH in mineral oil) gave imides **4** (80%), **7** (52%) and **8** (19%). *N*-methylferrocenecarboxamide (**5**) was prepared by a standard HOBt/EDC procedure by reaction of ferrocenecarboxylic acid (**1**) and methylamine [12].

Structural characterization of the novel ferrocene imides **4**, **7** and **8** was performed by IR, NMR spectroscopy and mass spectrometry. The NMR and IR spectra of imides **4** (Figures S1−S4), **7** (Figures S5−S8) and **8** Figures (S9−S13) are depicted in the Supporting Information. The IR spectra of all compounds are characterized by bands at ~1700 cm^{-1} attributable to symmetric and the antisymmetric C=O stretching vibrations of imide carbonyls, signals belonging to N−H stretching vibrations at ~3400 cm^{-1} as well as other bands characteristic for acyclic imides [42]. IR spectra of NH-region of imides **4**, **7** and **8** recorded in dichloromethane solutions ($c = 5 \times 10^{-2}$ mol dm^{-3}) contain bands belonging to free (above 3400 cm^{-1}) and hydrogen bonded (below 3400 cm^{-1}) NH groups (Figure 1 and Table 2, full IR spectra in Figures S3, S7 and S12). Since the intensity of the former bands is much stronger than that of the later, it can be assumed that the conformations with free NH groups dominate in the solutions of **4**, **7** and **8**, especially in the case of **8** in whose spectrum the signal below 3400 cm^{-1} is negligible. Moreover, the weak signals attributed to hydrogen-bonded NH groups of **4** and **7** decrease upon dilution due to dissociation of intermolecular hydrogen

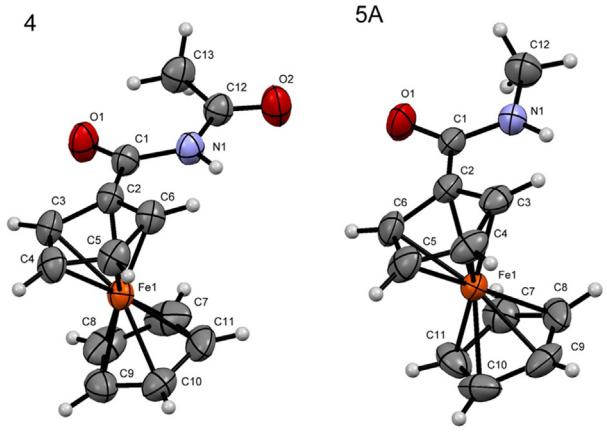

Figure 2. Molecular structures of **4** and **5A.** Thermal ellipsoids are drawn for the probability of 50 % and hydrogen atoms are depicted as spheres of arbitrary radii.

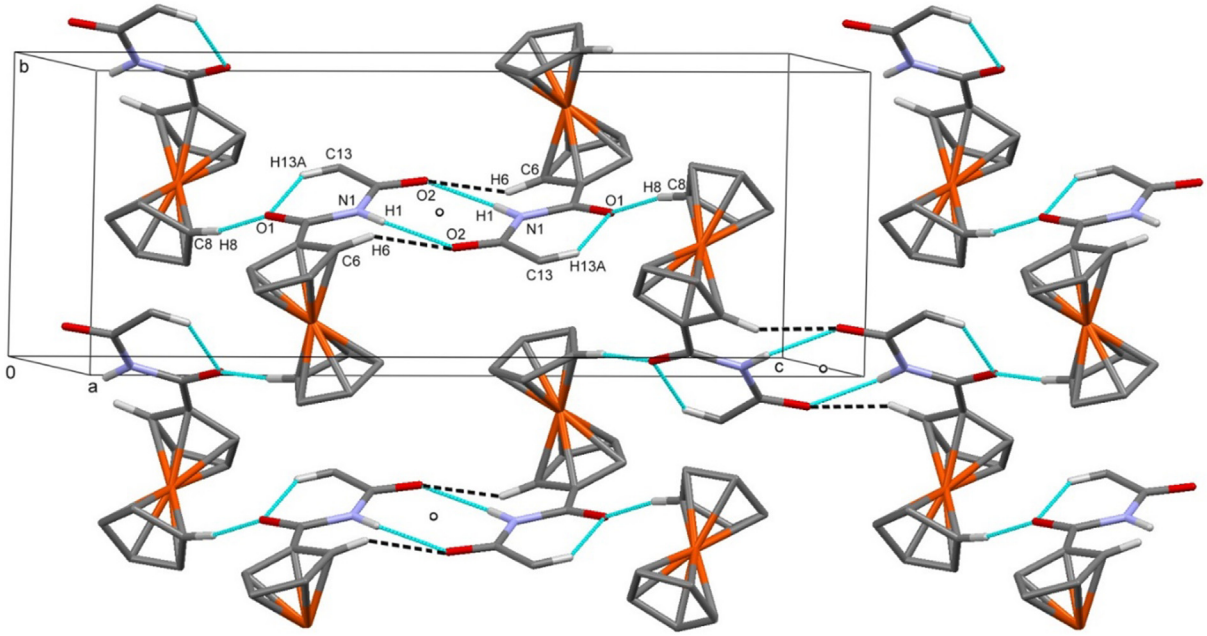

Figure 3. In crystal packing of **4** dimers are formed through centrosymmetric hydrogen bonded ring *via* a pair of symmetry-related N1−H1···O2 hydrogen bonds (crystallographic inversion centres are shown as black cirles). Dimers are connected through C8−H8···O1 hydrogen bonds along the direction [001] (above specified contacts are shown as turquoise lines), whereas the contact C6−H6···O2 completes the network in the plane (100) (shown as black dashed lines). Hydrogen atoms which do not participate in hydrogen bonding were omitted for clarity.

Table 4. Geometric parameters of hydrogen bonds.

	D−H/Å	H···*A*/Å	*D*···*A*/Å	*D*−H···*A*/°	Symm. op. on *A*
4					
N1−H1···O2	0.86	2.15	2.989 (3)	165	1–*x*, 1–*y*, 1–*z*
C6−H6···O2	0.93	2.50	3.255 (3)	138	1–*x*, 1–*y*, 1–*z*
C8−H8···O1	0.93	2.58	3.462 (4)	158	1–*x*, –1/2 + *y*, 1/2–*z*
C13−H13A···O1	0.96	2.04	2.808 (4)	136	*x*, *y*, *z*
5					
N1A−H1A···O1B	0.86	2.13	2.943 (4)	157	1–*x*, 1–*y*, 1–*z*
N1B−H1B···O1A	0.86	2.16	2.964 (4)	156	–*x*–1, 1–*y*, 1–*z*
C11B−H11B···O1A	0.93	2.71	3.488 (6)	142	–*x*, 1–*y*, 1–*z*
C9A−H9A···O1B	0.93	2.67	3.459 (6)	143	1–*x*, 1–*y*, 1–*z*
C3A−H3A···O1B	0.93	2.13	3.564 (7)	157	1–*x*, 1–*y*, 1–*z*

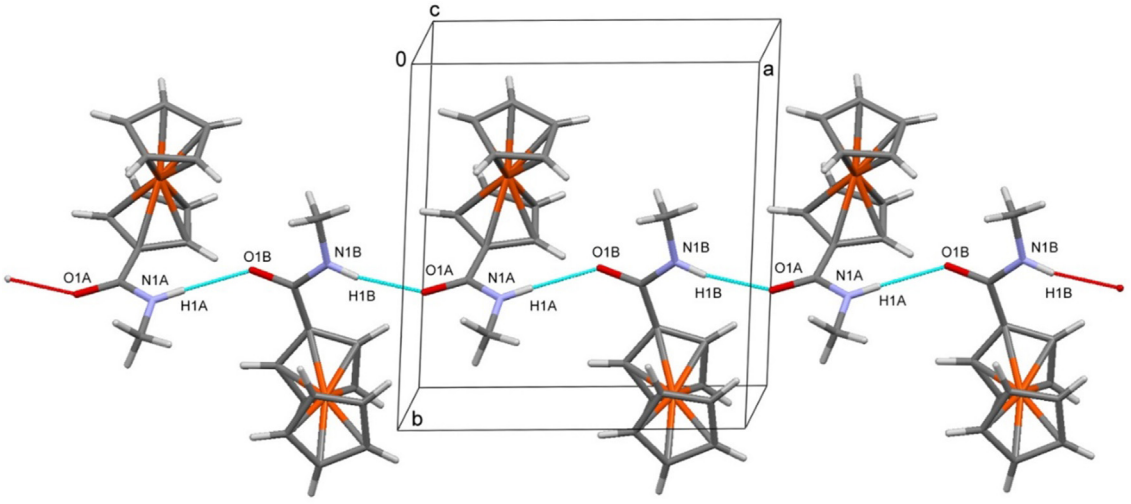

Figure 4. Crystal packing of **5** with hydrogen bond N−H···O (shown as turquoise lines) connecting crystalographically independent molecules A and B into a chain extending in the direction [100].

Table 5. Geometric parameters of the C–H···π interactions.

	H···Cg[a]/Å	C–H···Cg[a]/°	C···Cg[a]/Å	Symm. operation on Cg[a]
5				
C11A–H11A···C2A→C6A	3.00	151	3.845	$x, y, 1 + z$
C7A–H7A···C7B→C11B	3.48	151	4.325	$-x, -y, 1-z$
C13–H13···C8–C9–C10	3.08	161	3.969	$-1/2 + x, 3/2-y, z$
C9B–H9B···C2A→C6A	3.16	143	3.946	$x, -1+y, -1+z$

[a] Cg is the centre of gravity of the proton acceptor moiety.

bonds. In contrast, only the signals below 3400 cm^{-1}, belonging to the associated NH groups, are observed in the solid-state IR spectra of **4**, **7** and **8** (Table 2, Figures S4, S7 and S13). The NMR spectra of **4**, **7** and **8** showed all the expected signals which were assigned using NOE spectroscopy and coupling patterns. The signals of the NH groups of **4**, **7** and **8** are only slightly shifted to a higher field upon dilution, so it can be concluded that there is no significant aggregation in the concentration range studied, which is in agreement with IR spectroscopy.

3.2. Molecular structures and crystal packing of 4 and 5

The molecular and crystal structures of the compounds **4** and **5** (the latter comprising two molecules in an asymmetric unit, labelled as A and B, being the same conformer) (Figure 2) were determined by X-ray structure analysis revealing them as η^5-coordination π-complexes characterised by Fe^{II}–*Cp* bonds of 2.0242 (2)–2.061 (2) in **4**; 2.039 (3)–2.055 (4) Å (for molecule A) and 2.036 (5)–2.053 (5) Å (for molecule B) in **5**.

In both compounds C–C bonds of cyclopentadienyl rings are conjugated; for **4** bonds values are in the range: C2–C6 [1.416 (3)–1.441 (3) Å] and for C7–C11 [1.394 (4)–1.436 (5) Å]; for **5** C2A/C2B–C6A/C6B bonds values are in the range [1.415(4)/1.414(6)–1.433(5)/1.439(4) Å] and for C7A/C7B–C11A/C11B [1.405(6)/1.398(6)–1.422(6)/1.421(6) Å]. The cyclopentadienyl rings in both compounds are in an eclipsed conformation with related torsion angles C2–*Cp1*–*Cp2*–C7 [8.17°] for **4,** and [−12.69°] (molecule A) [−7.01°] (molecule B) in **5**.

Selected torsion angles defining the conformation of amide substituents in **4** and **5** relative to *Cp* rings are listed in Table 3. The conformation of amide substituent in **4** is defined by the two torsional angles: O1–C1–N1–C12 [7.6 (4)°] and O2–C12–N1–C1 [−179.7 (2)°]. The amide groups of **5** (molecules A and B) are planar with the mean value of deviations [0.004 (3) Å] from the best least-squares planes (defined by atoms C1, O1, N1, C12).

In synthesis of **4** and **5** racemic precursors were used and enantiomeric resolution has not occurred neither in syntheses nor for crystallization.

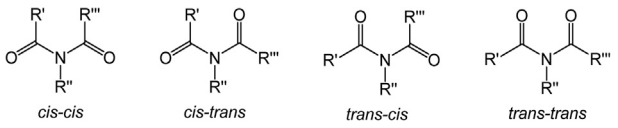

Figure 5. Four conformations of the imide group (R is H, cyclic or acyclic group). The stereochemical descriptors refer to the relative positions of the carbonyl groups with respect to the central N–R″ bond.

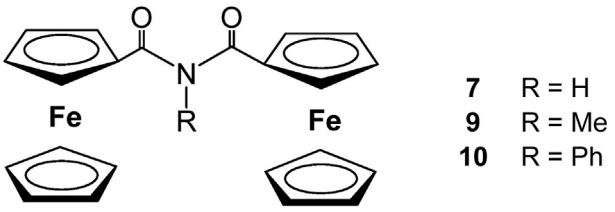

Figure 6. Compounds used in the conformational study.

In the crystal packing of **4** the main motif are hydrogen-bonded centrosymmetric dimers generated through a pair of symmetry-related hydrogen bonds N1–H1···O2 (forming an R^2_2 (8) motif; Figure 3, Table 4). Two C–H···O hydrogen bonds connect the dimers into layers parallel to the plane (100) (Figure 3, Table 4). The layers stack in the direction [001] and are connected by C–H···O interactions (2.78 Å) along [100] direction involving the ferrocene group and van der Waals forces.

Crystal packing of **5** is characterised by N–H···O hydrogen bonds connecting molecules A•••B•••A into a chain in the direction [100] (Figure 4, Table 4). The chains are further stabilised by C–H···O hydrogen bonding (2.79 Å) in the direction [001]. In other two directions, [100] and [010], the crystal is held together by van der Waals forces and C–H•••π interactions (Table 5). The hydrophilic chains are embedded into hydrophobic FeCp_2 regions and connected by C–H•••π interactions (Table 5).

3.3. Computational study

In theory, three imide groups (R′, R″ and R‴) can adopt four different conformations (Figure 5) differing in positions of the carbonyl groups relative to the substituent attached to nitrogen (R″). When two of these groups are the same (R′ = R‴) the number of different stereoisomers is reduced to three because *cis-trans* becomes equal to *trans-cis*. In previous studies the imide, R–CO–NH–CO–R system was usually considered as an amino group flanked by two carbonyls, and because of the resonance the free imide groups are essentially planar [13, 43]. The relative stability of different stereoisomers was further explained by the steric and electronic effects as follows. While *cis-cis* has the highest relative energy due to repulsion between two substituents (*R′* and *R″*), the *cis-trans* isomer is the most stable one and usually observed in solutions. The *trans-trans* conformer is less stable in comparison to *cis-trans* due to unfavourable repulsions between imide carbonyl groups.

To better explain the effect of the *N*-substituted imide nitrogen, in this paper we have focused on three different R″ groups (hydrogen in **7**, methyl in **9** and phenyl in **10**, Figure 6) attached to the imide nitrogen. Other two groups remain the same (Fc = R′ = R‴) in all three computationally

Table 6. List of the most stable conformers of **7**, **9** and **10**. Energy of each conformer was calculated relative to the energy of the most stable conformer from each series.

Label	*Stereochemical descriptor*	E_{rel}/kJ mol^{-1}
7–1	*cis-trans*	0.00
7–2	*cis-trans*	1.82
7–3	*trans-trans*	3.17
7–4	*cis-trans*	4.40
7–5	*cis-trans*	5.27
7-cc[a]	*cis-cis*	12.13
9–1	*cis-cis*	0.00
9–2	*cis-trans*	9.96
10–1	*cis-trans*	0.00
10–2	*cis-cis*	1.12
10–3	*trans-trans*	1.32
10–4	*trans-trans*	5.22

[a] some *cis-trans* conformers between **7-5** and **7-cc** were omitted from table.

investigated compounds. A relative distribution of the most contributing conformers in three dinuclear complexes was calculated in solvent (chloroform) modelled as polarizable continuum. Conformers are arranged in Figure 6 according to their relative energies. The conformational search methodology is explained in more details in section Computational details. It is based on three-step approach starting from the lowest level of theory (OPLS2005 force field, Monte Carlo conformational search algorithms) and only the representative sets of conformers were submitted further to full DFT optimizations in chloroform and verified as minima on the potential energy surface. We particularly chose chloroform based on our previous studies where computational data were tested against the NMR experiments to detect the most stable conformers [28, 29, 30, 31, 32, 33, 34, 35, 36, 37]. To simplify this study, trinuclear complexes were not individually analysed due to the fact that imide linkage between the second and the third ferrocene unit is assumed to be the same as between the first and the second ferrocene unit [12].

As expected, as the most stable conformers were found those with *cis-trans* relative orientation of the carbonyl groups relative to the *N*-substituted group for derivatives **7** and **10** (Table 6 and Figure 7) While there is preferentially only one such conformer below 5 kJ mol^{-1} characterized for phenyl substituted compound (e.g., **10-1**) there are at least three conformers of *cis-trans* configuration found for nonsubstituted imide **7**, mostly differing in a relative orientation of ferrocene units. In comparison with **10**, where phenyl can sterically interfere with nonsubstituted cyclopentadienyl ring, such interference is much weaker in compound **7** with small hydrogen atom on the imide group (e.g., **7-1**). Interestingly, *cis-cis* configuration was confirmed as the most stable for *N*-methyl substituted **9** while the energy gap between the first (*cis-cis*) and the second (*cis-trans*) conformer is about 10 kJ mol^{-1}, what corroborates previously published experimental data that *cis-cis* conformer of **9** is especially favourable in condensed phase. A very similar *cis-cis* configurations also exists in **7** with hydrogen, but it is one of the less

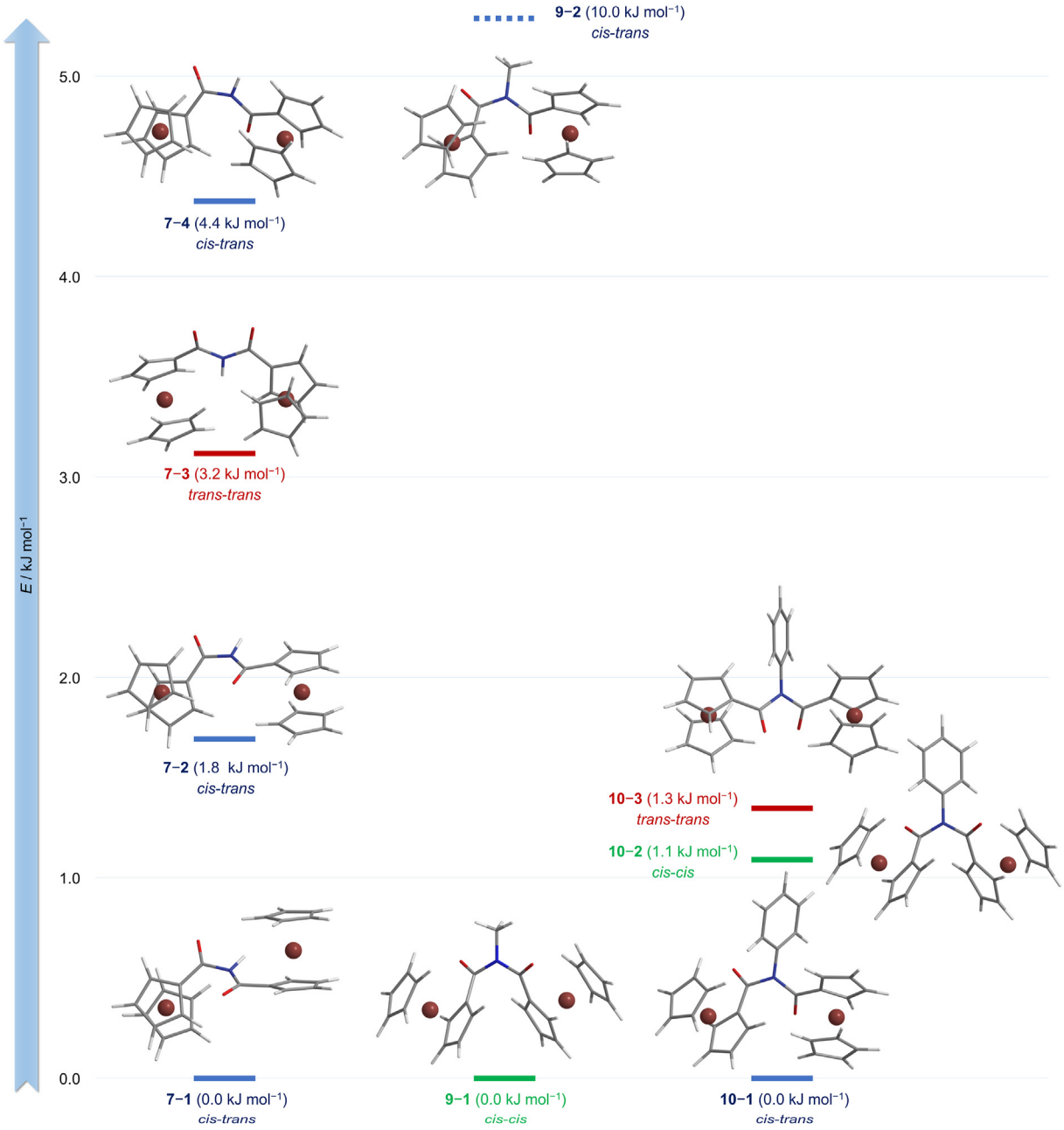

Figure 7. DFT optimized geometries of the most stable conformers of imide *N*-substituted bis-ferrocene derivatives **7** (R = H), **9** (R = Me) and **10** (R = Ph). Relative energies (in kJ mol^{-1}) are displayed in parenthesis after the labels.

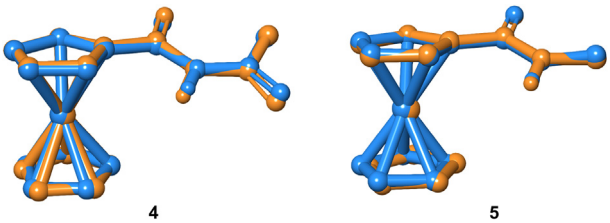

Figure 8. Superposition of two geometries, X-ray determined crystal structures are coloured in blue and geometries of the most stable conformers are coloured in orange. The calculated RMSD values are 0.145 Å for **4** and 0.057 Å for **5**.

stable conformers with relative energy of about 12 kJ mol^{-1}. In comparison, all three configurations (*cis-cis*, *cis-trans* and *trans-trans*) are energetically very close in **10** with bulkier Ph group.

All of the so far reported X-ray determined crystal structures with *N*-methyl [12], *N*-phenyl [18] and *N*-pyridyl [19, 20] preferentially show *cis-cis* orientation. There is a perfect match between the experimental [12] and in solution and in the solid state determined conformers of *N*-methyl **9**, i.e., the most abundant conformers adopt *cis-cis* configurations. However, some differences were observed between the experimental [18] and computationally confirmed conformers of *N*-phenyl **10**. The relative energy difference between all three possible conformers is quite small in **10** and the preference for *cis-cis* in the solid state can be partially explained by stabilizing intermolecular interactions. Unfortunately, we were not able to determine crystal structure of **7**.

In addition, to test the validity of the conformational search approach, we have also performed conformational analysis of derivatives **4** and **5**. Geometries of the most stable conformers optimized in solution match well with those determined in the solid state. The calculated root mean square deviations (RMSDs) are only 0.145 Å for **4** and 0.057 Å for **5** (Figure 8).

4. Conclusion

In this research, we presented the synthesis and spectroscopic analysis of aromatic imides possessing one (**4**), two (**7**) and three (**8**) ferrocene units connected with iminodicarbonyl linkers, as well as the crystal structures of *N*-methylferrocenecarboxamide (**5**) and *N*-acetylferrocenecarboxamide (**4**). Compounds Fc−CO−NH−CO−Me (**4**), Fc−CO−NH−CO−Fc (**7**) and Fc−CO−NH−CO−Fn−CO−NH−CO−Fc (**8**) were prepared by amidation reactions starting from the corresponding ferrocenecarbonyl chlorides or acetyl chloride and ferrocenecarboxamide. The NH-region of the IR spectra of imides **4**, **7** and **8**, taken in diluted solutions of nonpolar solvent, is dominated by signals above 3400 cm^{-1} indicating the absence of intramolecular hydrogen-bonding. Since the chemical shifts of the NH groups in the ^{1}H NMR spectra of imides **4**, **7** and **8** are almost independent of concentration, it can be concluded that there is no significant aggregation in the concentration range studied. X-ray crystal structure analysis showed that N−H···O hydrogen bonds associate the molecules of **4** in centrosymmetric dimers, and the molecules of its homologue *N*-methylferrocenecarboxamide (**5**) are self-assembled by intermolecular N−H···O bonds into infinite chains. A detailed conformational analysis suggests the dominance of *cis-trans* configurations of **7** in solution. In addition, we have investigated the effect of different *N*-substituents (methyl and phenyl) on a relative distribution of bis-ferrocenyl imide bridged compounds and confirmed matching with the experimental data.

Declarations

Author contribution statement

Mojca Čakić Semenčić, Ivan Kodrin: Conceived and designed the experiments; Performed the experiments; Analyzed and interpreted the data; Contributed reagents, materials, analysis tools or data; Wrote the paper.

Krešimir Molčanov, Monika Kovačević: Performed the experiments; Analyzed and interpreted the data; Contributed reagents, materials, analysis tools or data.

Vladimir Rapić: Contributed reagents, materials, analysis tools and data.

Funding statement

This work was supported by the Ministry of Science, Education and Sports of The Republic of Croatia (Grant Number 058-1191344-3122) and funding from the Croatian Academy of Sciences and Arts to I.K.

Data availability statement

Data included in article/supplementary material/referenced in article.

Declaration of interests statement

The authors declare the following conflict of interest: Ivan Kodrin is a member of the advisory board for Heliyon (section: Heliyon Chemistry).

Additional information

Supplementary content related to this article has been published online at https://doi.org/10.1016/j.heliyon.2022.e09470.

References

[1] F.D. Lewis, T.L. Kurth, C.M. Hattan, R.C. Reiter, C.D. Stevenson, Polyaryl anion radicals via alkali metal reduction of arylurea oligomers, Org. Lett. 6 (2004) 1605–1608.
[2] M. Kudo, A. Tanatani, Conformational properties of aromatic multi-layered and helical oligoureas and oligoguanidines, New J. Chem. 39 (2015) 3190–3196.
[3] R. Liu, A.L. Connor, F.Y. Al-mkhaizim, B. Gong, Aromatic oligoamides with increased backbone flexibility: improved synthetic efficiencies, solvent-dependent folding and cooperative conformational transitions, New J. Chem. 39 (2015) 3217–3220.
[4] I. Huc, Aromatic oligoamide foldamers, Eur. J. Org Chem. 2004 (2004) 17–29.
[5] M. Pasco, C. Dolain, G. Guichard, Foldamers in medicinal chemistry, in: Compr. Supramol. Chem. II, Elsevier, 2017, pp. 89–125.
[6] G. Guichard, I. Huc, Synthetic foldamers, Chem. Commun. 47 (2011) 5933.
[7] S. Kohmoto, H. Takeichi, K. Kishikawa, H. Masu, I. Azumaya, Conformation of S-shaped aromatic imide foldamers and their induced circular dichroism, Tetrahedron Lett. 49 (2008) 1223–1227.
[8] H. Masu, I. Mizutani, T. Kato, I. Azumaya, K. Yamaguchi, K. Kishikawa, S. Kohmoto, Naphthalene- and anthracene-based aromatic foldamers with iminodicarbonyl linkers: their stabilities and application to a chiral photochromic system using retro [4 + 4] cycloaddition, J. Org. Chem. 71 (2006) 8037–8044.
[9] H. Masu, I. Mizutani, Y. Ono, K. Kishikawa, I. Azumaya, K. Yamaguchi, S. Kohmoto, Phase-dependent emission of Naphthalene−Anthracene-based concave-shaped molecules, Cryst. Growth Des. 6 (2006) 2086–2091.
[10] H. Masu, K. Ohmori, K. Kishikawa, M. Yamamoto, K. Yamaguchi, S. Kohmoto, Crystal structures of aromatic chain imides possessing a concave-shaped conformation, Anal. Sci. X-Ray Struct. Anal. Online. 21 (2005) X33–X34.
[11] H. Masu, M. Sakai, K. Kishikawa, M. Yamamoto, K. Yamaguchi, S. Kohmoto, Aromatic foldamers with iminodicarbonyl linkers: their structures and optical properties, J. Org. Chem. 70 (2005) 1423–1431.
[12] V. Kovač, M.Č. Semenčić, K. Molčanov, I. Sabljić, D. Iveković, M. Žinić, V. Rapić, Synthesis and structure of bis- and tris-ferrocene containing N-methylimide foldamers, Tetrahedron 68 (2012) 7884–7891.
[13] M.C. Etter, D. Britton, S.M. Reutzel, Structures of N-acetylbenzamide, N-propionylbenzamide and N-butyrylbenzamide and analysis of imide hydrogen-bond patterns, Acta Crystallogr. Sect. C Cryst. Struct. Commun. 47 (1991) 556–561.
[14] S.M. Reutzel, M.C. Etter, Evaluation of the conformational, hydrogen bonding and crystal packing preferences of acyclic imides, J. Phys. Org. Chem. 5 (1992) 44–54.
[15] A. Saeed, M.F. Erben, M. Bolte, Twisted imide bond in noncyclic imides. Synthesis and structural and vibrational properties of N , N -Bis(furan-2-carbonyl)-4-chloroaniline, J. Org. Chem. 77 (2012) 4688–4695.
[16] A. Saeed, T. Hökelek, M. Bolte, M.F. Erben, Intra- and intermolecular N–H•••O=C hydrogen bonds in 1-acyl urea compounds: synthesis, X-ray structure, conformational and Hirshfeld surface analyses of 1-(2,3-dichlorophenyl)-3-pivaloylurea, J. Mol. Struct. 1245 (2021) 131271.
[17] M.V. Il'in, L.A. Lesnikova, D.S. Bolotin, A.S. Novikov, V.V. Suslonov, V.Y. Kukushkin, A one-pot route to: N -acyl ureas: a formal four-component hydrolytic reaction involving aminonitrones and isocyanide dibromides, New J. Chem. 44 (2020) 1253–1262.

[18] F. Zhao, G. Li, J.-X. Wu, Z.-P. Zhang, Jiegou Huaxue 26 (2007) 291. http://manu30.magtech.com.cn/jghx/EN/article/showTenYearOldVolumn.do.
[19] T. Moriuchi, T. Hirao, Imide-bridged diferrocene for protonation-controlled regulation of electronic communication, Tetrahedron Lett. 48 (2007) 5099–5101.
[20] S. Quintal, S. Fedi, J. Barbetti, P. Pinto, V. Félix, M.G.B. Drew, P. Zanello, M.J. Calhorda, Synthesis and properties of new Mo(II) complexes with N-heterocyclic and ferrocenyl ligands, J. Organomet. Chem. 696 (2011) 2142–2152.
[21] H.-J. Lorkowski, R. Pannier, A. Wende, Über Ferrocenderivate. VIII. Die Darstellung von monomeren und polymeren Ferrocenylenoxadiazolen, J. Prakt. Chem. 35 (1967) 149–158.
[22] F.W. Knobloch, W.H. Rauscher, Condensation polymers of ferrocene derivatives, J. Polym. Sci. 54 (1961) 651–656.
[23] L. Barišić, M. Čakić, K.A. Mahmoud, Y. Liu, H.-B. Kraatz, H. Pritzkow, S.I. Kirin, N. Metzler-Nolte, V. Rapić, Helically chiral ferrocene peptides containing 1′-aminoferrocene-1-carboxylic acid subunits as turn inducers, Chem. Eur J. 12 (2006) 4965–4980.
[24] O.D. Rigaku, P.R.O. CrysAlis, Rigaku Oxford Diffraction Ltd, Yarnton, England, 2018.
[25] G.M. Sheldrick, SHELXT – integrated space-group and crystal-structure determination, Acta Crystallogr. Sect. A Found. Adv. 71 (2015) 3–8.
[26] A.L. Spek, checkCIF validation ALERTS: what they mean and how to respond, Acta Crystallogr. Sect. E Crystallogr. Commun. 76 (2020) 1–11.
[27] C.F. Macrae, I.J. Bruno, J.A. Chisholm, P.R. Edgington, P. McCabe, E. Pidcock, L. Rodriguez-Monge, R. Taylor, J. van de Streek, P.A. Wood, Mercury CSD 2.0 – new features for the visualization and investigation of crystal structures, J. Appl. Crystallogr. 41 (2008) 466–470.
[28] M. Nuskol, P. Šutalo, I. Kodrin, M.Č. Semenčić, Sensing of the induced helical chirality by the chiroptical response of the ferrocene chromophore, Eur. J. Inorg. Chem. 2022 (2022).
[29] M. Kovačević, M. Čakić Semenčić, K. Radošević, K. Molčanov, S. Roca, L. Šimunović, I. Kodrin, L. Barišić, Conformational preferences and antiproliferative activity of peptidomimetics containing methyl 1′-Aminoferrocene-1-carboxylate and turn-forming homo- and heterochiral pro-ala motifs, Int. J. Mol. Sci. 22 (2021) 13532.
[30] M. Nuskol, P. Šutalo, M. Đaković, M. Kovačević, I. Kodrin, M. Čakić Semenčić, Testing the potential of the ferrocene chromophore as a circular dichroism probe for the assignment of the screw-sense preference of tripeptides, Organometallics 40 (2021) 1351–1362.
[31] M. Nuskol, B. Studen, A. Meden, I. Kodrin, M. Čakić Semenčić, Tight turn in dipeptide bridged ferrocenes: synthesis, X-ray structural, theoretical and spectroscopic studies, Polyhedron 161 (2019).
[32] M. Kovačević, I. Kodrin, S. Roca, K. Molčanov, Y. Shen, B. Adhikari, H.-B. Kraatz, L. Barišić, Helically chiral peptides that contain ferrocene-1,1′-diamine scaffolds as a turn inducer, Chem. Eur J. 23 (2017).
[33] M. Čakić Semenčić, I. Kodrin, L. Barišić, M. Nuskol, A. Meden, Synthesis and conformational study of monosubstituted aminoferrocene-based peptides bearing homo- and heterochiral pro-ala sequences, Eur. J. Inorg. Chem. 2017 (2017).
[34] M. Kovačević, I. Kodrin, M. Cetina, I. Kmetič, T. Murati, M.C. Semenčić, S. Roca, L. Barišić, The conjugates of ferrocene-1,1′-diamine and amino acids. A novel synthetic approach and conformational analysis, Dalton Trans. 44 (2015).
[35] M.C. Semenčić, V. Kovač, I. Kodrin, L. Barišić, V. Rapić, Synthesis and conformational study of bioconjugates derived from 1-acetyl-1′-aminoferrocene and α-amino acids, Eur. J. Inorg. Chem. 2015 (2015).
[36] V. Kovač, M. Čakić Semencic, I. Kodrin, S. Roca, V. Rapić, Ferrocene-dipeptide conjugates derived from aminoferrocene and 1-acetyl-1′-aminoferrocene: synthesis and conformational studies, Tetrahedron 69 (2013).
[37] L. Barišić, M. Kovačević, M. Mamić, I. Kodrin, Z. Mihalić, V. Rapić, Synthesis and conformational analysis of methyl N-alanyl-1′- aminoferrocene-1-carboxylate, Eur. J. Inorg. Chem. (2012).
[38] LLC, New York, NY, Macro Model, Schrödinger, 2019.
[39] F. Mohamadi, N.G.J. Richards, W.C. Guida, R. Liskamp, M. Lipton, C. Caufield, G. Chang, T. Hendrickson, W.C. Still, Macromodel - an integrated software system for modeling organic and bioorganic molecules using molecular mechanics, J. Comput. Chem. 11 (1990) 440–467.
[40] M.J. Frisch, G.W. Trucks, H.B. Schlegel, G.E. Scuseria, M.a. Robb, J.R. Cheeseman, G. Scalmani, V. Barone, G.a. Petersson, H. Nakatsuji, X. Li, M. Caricato, a.V. Marenich, J. Bloino, B.G. Janesko, R. Gomperts, B. Mennucci, H.P. Hratchian, J.V. Ortiz, a.F. Izmaylov, J.L. Sonnenberg, Williams, F. Ding, F. Lipparini, F. Egidi, J. Goings, B. Peng, A. Petrone, T. Henderson, D. Ranasinghe, V.G. Zakrzewski, J. Gao, N. Rega, G. Zheng, W. Liang, M. Hada, M. Ehara, K. Toyota, R. Fukuda, J. Hasegawa, M. Ishida, T. Nakajima, Y. Honda, O. Kitao, H. Nakai, T. Vreven, K. Throssell, J.a. Montgomery Jr., J.E. Peralta, F. Ogliaro, M.J. Bearpark, J.J. Heyd, E.N. Brothers, K.N. Kudin, V.N. Staroverov, T.a. Keith, R. Kobayashi, J. Normand, K. Raghavachari, a.P. Rendell, J.C. Burant, S.S. Iyengar, J. Tomasi, M. Cossi, J.M. Millam, M. Klene, C. Adamo, R. Cammi, J.W. Ochterski, R.L. Martin, K. Morokuma, O. Farkas, J.B. Foresman, D.J. Fox, Gaussian 16, Revision C.01, 2016.
[41] K. Schlögl, Über Ferrocen-Aminosäuren und verwandte Verbindungen, Monatsh. Chem. 88 (1957) 601–621.
[42] T. Uno, K. Machida, Infrared spectra of acyclic imides. II. The characteristic absorption bands of saturated acyclic imides in the crystalline state, Bull. Chem. Soc. Jpn. 34 (1961) 551–556.
[43] R.D. Parra, M. Furukawa, B. Gong, X.C. Zeng, Energetics and cooperativity in three-center hydrogen bonding interactions. I. Diacetamide-X dimers (X=HCN, CH3OH), J. Chem. Phys. 115 (2001) 6030–6035.